Biogeosciences Discuss., 12, 18007–18051, 2015
www.biogeosciences-discuss.net/12/18007/2015/
doi:10.5194/bgd-12-18007-2015

Biogeosciences Discussions
Open Access
EGU

Combining multi-spectral proximal sensors and digital cameras for monitoring grazed tropical pastures

R. N. Handcock[1,a], D. L. Gobbett[2], L. A. González[3,b], G. J. Bishop-Hurley[4], and S. L. McGavin[3]

[1]Commonwealth Scientific and Industrial Research Organisation (CSIRO), Agriculture, Private Bag 5, Floreat, WA, 6014, Australia
[2]CSIRO Agriculture, PMB 2, Glen Osmond, SA, 5064, Australia
[3]CSIRO Agriculture, PMB Post Office, Aitkenvale, QLD, 4814, Australia
[4]CSIRO Agriculture, 306 Carmody Rd., St Lucia, QLD, 4067, Australia
[a]now at: Murdoch University, 90 South St., Murdoch, WA, 6150, Murdoch, WA, Australia
[b]now at: Faculty of Agriculture and Environment, Centre for Carbon, Water and Food, The University of Sydney, 380 Werombi Rd., Camden, NSW, 2570, Australia

Received: 30 June 2015 – Accepted: 13 October 2015 – Published: 11 November 2015

Correspondence to: R. N. Handcock (r.handcock@murdoch.edu.au)

Published by Copernicus Publications on behalf of the European Geosciences Union.

Abstract

Timely and accurate monitoring of pasture biomass and ground-cover is necessary in livestock production systems to ensure productive and sustainable management of forage for livestock. Interest in the use of proximal sensors for monitoring pasture status in grazing systems has increased, since such sensors can return data in near real-time, and have the potential to be deployed on large properties where remote sensing may not be suitable due to issues such as spatial scale or cloud cover. However, there are unresolved challenges in developing calibrations to convert raw sensor data to quantitative biophysical values, such as pasture biomass or vegetation ground-cover, to allow meaningful interpretation of sensor data by livestock producers. We assessed the use of multiple proximal sensors for monitoring tropical pastures with a pilot deployment of sensors at two sites on Lansdown Research Station near Townsville, Australia. Each site was monitored by a Skye SKR-four-band multi-spectral sensor (every 1 min), a digital camera (every 30 min), and a soil moisture sensor (every 1 min), each operated over 18 months. Raw data from each sensor were processed to calculate a number of multispectral vegetation indices. Visual observations of pasture characteristics, including above-ground standing biomass and ground cover, were made every 2 weeks. A methodology was developed to manage the sensor deployment and the quality control of the data collected. The data capture from the digital cameras was more reliable than the multi-spectral sensors, which had up to 63 % of data discarded after data cleaning and quality control. We found a strong relationship between sensor and pasture measurements during the wet season period of maximum pasture growth (January to April), especially when data from the multi-spectral sensors were combined with weather data. RatioNS34 (a simple band ratio between the near infrared (NIR) and lower shortwave infrared (SWIR) bands) and rainfall since 1 September explained 91 % of the variation in above-ground standing biomass (RSE = 593 kg DM ha^{-1}, $p < 0.01$). RatioNS34 together with rainfall explained 95 % of the variation in the percentage of green vegetation observed in 2-dimensions (%Green2D) (RSE = 6 %, $p < 0.01$). The Green Leaf Algo-

BGD
12, 18007–18051, 2015

rithm index derived from the digital camera images and the rainfall accumulated since the 1 September explained 91 % of the variation in %Green2D (RSE = 9 %, $p < 0.01$, df = 20), but had a poor relationship with biomass. Although proximal sensors observe only a small area of the pasture, they deliver continual and timely pasture measurements to inform timely decision-making on-farm.

1 Introduction

Frequent and accurate monitoring of pastures in livestock production systems is necessary to facilitate timely and appropriate management decisions. Traditional methods for measuring pasture biomass (e.g. pasture cuts, visual assessments and plate meters), (Sanderson et al., 2001) are time-consuming and error-prone, leading to an increased interest in automated monitoring methods. While remote sensing of the landscape from satellite-based platforms gives extensive spatial coverage, its usefulness can be limited by irregular availability of suitable images, which in tropical environments can be further restricted by cloud cover, particularly during the wet season. Converting raw satellite images to a measure that is useful for on-farm decision making is also problematic due to the cost and processing requirements for operational delivery (e.g. Handcock et al., 2008). Continual monitoring using proximal sensors has the advantage over satellite images of capturing rapid-changes in the proportions of photosynthetically-active vegetation (PV) (i.e. green) and non photosynthetically-active vegetation (NPV) (i.e. dead/dry). Such changes in the feed-base can signal that farm-management interventions are necessary for better utilization of resources and reducing detrimental environmental impacts due to overgrazing. For example, at the end of the wet season in tropical environments, beef producers need to assess how much green feed remains in the paddocks to determine if there is sufficient feed to carry the cattle through the dry season, or to adjust stocking rates accordingly (O'Reagain et al., 2014), provide supplemental feed, or move animals.

BGD
12, 18007–18051, 2015

With recent advances in wireless sensor networks and improved mobile network coverage, the delivery of monitoring data from sensors in remote cattle enterprises in a near-real time data stream has become feasible. While proximal sensors monitor a small area or point and do not provide the extensive coverage of satellite imagery, when strategically placed within the farm these sensors have the potential to deliver continual data on the feed-base and allow more responsive management decisions.

In the present study, proximal sensors refer to in-situ sensors placed within several metres of the surface to be monitored, or placed in the shallow sub-surface environment, and providing repeat measurements at discrete intervals over periods of days to years. This distinguishes fixed proximal sensors from those which are mobile via robotic or aerial platforms (e.g. Von Bueren et al., 2015; Hamilton et al., 2007), vehicle-mounted sensors (e.g. King et al., 2010), or hand-held such as a field spectroradiometer (e.g. Peddle et al., 2001). While each of these moveable sensor types has their own advantages, such as covering large areas for the mobile sensors, or in targeted measurements in the case of hand-held sensors, none have the ability for easy long temporal coverage which is provided by fixed proximal sensors. Proximal sensors are of particular interest in extensive grazing enterprises in remote regions where access to repeat monitoring is costly and difficult, yet where remote sensing is not suitable due to issues such as scale or cloud cover.

There has been recent growth in the use of in-situ proximal environmental sensors for a wide range of monitoring, including soils (Allen et al., 2007; Zerger et al., 2010) and ecological studies (Collins et al., 2006; Hamilton et al., 2007; Szewczyk et al., 2004), temperate pastures (Zerger et al., 2010; Gobbett et al., 2013), forests (Eklundh et al., 2011), and sub-alpine grasslands (Sakowska et al., 2014), or to complement measurements made from flux towers (Balzarolo et al., 2011; Gamon, 2015). Networks to support the improvement of such sensors have recently been developed, such as through SpecNet (http://specnet.info), and the projects presented in the current special issue.

BGD
12, 18007–18051, 2015

With minimal processing, the data obtained from sensors, such as spectral reflectance, can be related to biophysical values and provide useful qualitative information. An example is the well-established field of multi-spectral sensing using vegetation indices (e.g. Tucker, 1979). Vegetation indices are frequently calibrated to the biophysical properties of the vegetation such as leaf area index (Turner et al., 1999), biomass (Pearson et al., 1976; Handcock et al., 2008), percentage vegetation cover (Lukina et al., 1999), or the fraction of photosynthetically active radiation absorbed by a canopy (Richardson et al., 2007; Myneni and Williams, 1994; Guerschman et al., 2009). Converting sensor data to quantitative biophysical values such as pasture biomass and groundcover, allows easier interpretation of the sensor data for making management decisions by livestock producers.

The aim of this study was to quantify how well multiple proximal sensors could be used to monitor tropical pasture biomass, which requires both obtaining reliable data, and calibrating that data to biophysical values. To address this goal we assessed how the relationships between sensor and field observations of pastures differed between the wet and dry seasons in a tropical pasture grazed by cattle. The multi-spectral sensor data were calibrated using repeated visual observations of pasture characteristics supplemented by data from digital cameras, soil moisture sensors and weather data. We also developed methods for the management of multiple proximal sensors deployed for pasture monitoring in a tropical environment and the quality control of such data which extends on previous work in temperate pastures (Gobbett et al., 2013).

2 Methods

2.1 Field site and sensor nodes

The sensors deployed in this study were located at the Commonwealth Scientific and Industrial Research Organisation's (CSIRO) Lansdown Research Station near Townsville, Queensland, Australia (19°39′42″ S and 146°51′12″ E, elevation 63 m).

BGD
12, 18007–18051, 2015

Paddocks used in this study contained pastures dominated by *Urochloa* spp., *Chloris* spp., and *Stylosanthes* spp. Data were collected over 545 days between 23 September 2011 and 21 March 2013.

Based on daily precipitation and temperature data collected by the Bureau of Meteorology (BoM) from the "Woolshed" station (approximately 45 km NW of the study site) the tropical climate in the study region is characterised by a wet-season from November to April where monsoonal storms bring intermittent periods of heavy rainfall, and a winter dry-season with little or no rainfall. The average annual rainfall of 1139 mm falls mainly during the wet season, and the average monthly temperatures range is 20.8 to 28.5 °C in January, and 10.4 to 21.8 °C in July.

Two identical sensor nodes (Fig. 1) were mounted with the same array of equipment (multi-spectral sensors, digital camera, soil moisture sensor, wireless networking infrastructure), and providing spatially-coincident data with both high temporal- and spatial-resolution. The nadir-pointing sensors were located at a height of 2.5 m above the ground. At this height the downward-pointing multi-spectral sensor had a 25° field of view (FOV) sensing approximately 0.97 m^2 of area at ground level, although this area changes across the season as the vegetation height changes. See Balzarolo et al. (2011) for a discussion of optical sensor configurations.

The nodes were approximately 200 m apart in areas of the paddock visually assessed to be uniform and similar at the time of installation. One node was unfenced, permitting access to the area under the node by cattle grazing in the paddock. The second node was enclosed by a 30 m by 30 m fence which excluded cattle from grazing within the enclosure, but allowed access by kangaroos and other small herbivores. Each node included a solar-powered sensor hub which relayed captured sensor data to a wireless sensor network (WSN) installed on the research farm, and via an internet connection to a centralized enterprise database. All equipment was temporarily removed for a week during a controlled property burn in mid-December 2011.

BGD
12, 18007–18051, 2015

2.2 Soil moisture sensors

A Decagon "5TM" soil moisture sensor (Decagon Devices, USA) was installed to monitor the volumetric water content (VWC) of the soil. The VMC is the volume of water per unit of total volume, determined by measuring the dielectric constant of the soil, as well as soil temperature from a thermistor. The 5TM sensors were buried at a depth of 15 cm under the soil surface below the multi-spectral sensors. This depth was used to capture soil moisture near the surface, yet reduce the possibility of damage from trampling by cattle. The 5TM sensors recorded soil moisture and soil temperature readings at 1 min intervals. We extracted an average of VMC for the period between 12:00 and 13:00 for each day, resulting in a time series of daily VWC (i.e. SoilMoisture) and soil temperature data during the study period.

2.3 Weather data

The nearest BoM weather stations were at "Woolshed", "Charters Towers Airport" (both inland), and "Townsville Airport" (coastal), approximately 45 km NW, 70 km SW and 40 km N of the study site, respectively. Daily maximum ambient temperature averaged for the two inland stations had a strong relationship with temperature data from 12:00 from the 5TM soil moisture sensor, so these datasets were used interchangeably. The 5TM soil moisture sensors were additionally used as the main source of soil moisture data.

At the time of this study a new meteorological station at the Lansdown Research Station had recently been installed, but the data were not available for the study period. Given the spatial heterogeneity of precipitation events, the nationally available interpolated climate surfaces from BoM were thought to be too coarse for our small study site. A comparison of data from nearby BoM stations with the in-situ soil moisture sensors at our nodes showed a strong correlation with the average of the precipitation recorded at "Charters Towers Airport" and "Townsville Airport" stations, so this station average precipitation was used as the best of the available options for precipitation.

BGD
12, 18007–18051, 2015

The start and end of the wet season was determined using a method designed for the North Australian climate (Lo et al., 2007) in which the start of the wet season is defined as the date after 1 September when 50 mm of precipitation has accumulated. Bureau of Meteorology precipitation data from the "Townsville Airport" station were used to define the start and end of the wet and dry seasons, as this station had the most complete time-series of the nearby stations. Using this method, the 2011/12 wet season at our study site started on the 5 December 2011, and the 2012/13 wet season started on 1 January 2013.

2.4 Digital cameras and the VegMeasure semi-automated classification

Digital cameras were deployed at the study site to provide an automated assessment of ground cover (see Zerger et al., 2012), to serve as a visual cross-check of the multi-spectral data, and to assist in identifying surface water. At each of the two nodes we deployed a Pentax Optio WG-1 digital camera in a downward-pointing position that imaged the same FOV as the multi-spectral sensors. This model camera was selected as it was inexpensive, weatherproof and had an inbuilt intervalometer to enable automatic shooting at fixed intervals. At 2.5 m the 13.8 megapixel digital cameras recorded images with an approximate 0.6 mm ground resolution. The cameras were configured with flash off, sensitivity at ISO 200, autofocus and automatic white balance enabled. Digital images (approximately 1 to 4 MB each) were captured every 30 min and were manually downloaded at approximately 2-week intervals.

The images from the cameras contained un-calibrated red, green and blue (RGB) spectral bands. There has been extensive work on automated and semi-automated classification of such time series of digital photographs for the purposes of vegetation monitoring (e.g. Ewing and Horton, 1999; Karcher and Richardson, 2005; Bennett et al., 2000). As the focus of the current study was on the calibration of the multi-spectral sensor data, we chose to use a semi-automated method, VegMeasure (Johnson et al., 2003), to extract a green cover fraction of the time-series of digital camera images from each node. VegMeasure has been utilized and validated in a number of

BGD
12, 18007–18051, 2015

studies (e.g. Booth et al., 2005; Louhaichi et al., 2001) and provides a rapid method to classify a series of images into green and non-green using the Green Leaf Algorithm (GLA). The GLA applies the following spectral band ratio (Louhaichi et al., 2001):

$$\frac{(G-R)+(G-B)}{(G+R+G+B)}. \quad (1)$$

where G is the digital number of the green band, R is the digital number of the red band and B is the digital number of the blue band. The proportion of the pixels in each image in which the band ratio exceeds a user defined threshold is reported as the GLA.

For each day in the study period, the camera image taken nearest in time to 12:00 was selected, and the time-series was quality controlled for days when there was site maintenance work under the node. One photo with a mix of PV (i.e. green) and NPV vegetation was manually selected as a calibration image (14 May 2012, 12:13:55 GMT, on the unfenced node). To derive a threshold value for the GLA, one hundred random points were manually assigned to two classes: "white" = green vegetation and "black" = non-green vegetation background material including litter and soil). The resulting GLA threshold of 0.095 was verified using a random selection of images and used to process all images to extract the green proportion. The GLA was used as a crosscheck of the green fraction determined from the multi-spectral dataset and from field measurement.

2.5 Multi-spectral sensors

We used a paired sensor setup (Fig. 1) with the downward-pointing sensor having a conical field of FOV of 25°, allowing it to sense reflected light only from the ground directly beneath the sensor. The upward-pointing sensor was fitted with a cosine diffusing filter to alter its FOV to a full hemispherical view, permitting the albedo of the surface to be assessed relative to the incident solar radiation. Sensors were checked and cleaned fortnightly and the sensor station coated with insecticide to deter crawling and flying insects.

BGD
12, 18007–18051, 2015

The multispectral sensors mounted on each of the two nodes were paired Skye SKR-1850 four-band weatherproof sensors (Skye-Instruments, 2012a) configured with bands in the green (0.545 to 0.547 µm), red (0.644 to 0.646 µm), near infrared (NIR) (0.834 to 0.837 µm) and the lower SWIR (1.028 to 1.029 µm) spectral range (wavelengths in brackets indicate band widths). These bands were chosen as the NIR band is widely used in monitoring vegetation "greenness" from multispectral sensors (Tucker, 1979), and the SWIR region of the electromagnetic spectrum is sensitive to plant moisture content (Tucker, 1980). Additionally, these bands were chosen as both the SWIR and upper NIR spectral data can be used to help differentiate PV from both NPV and soil (Asner, 1998), and broad-band SWIR indices have been used to capture seasonally-varying NPV proportions resulting from repeat grazing of pastures by livestock (Handcock et al., 2008).

2.6 Vegetation indices

Spectral bands in the NIR region are commonly used to calculate a large range of vegetation indices, such as the normalized difference vegetation index (NDVI) (Tucker, 1979). A variety of vegetation indices are possible from combinations of these four broad spectral bands, some of which have become used for specific applications. However, due to the complexity of calculating indices from this particular Skye sensor model (see below), our index choice was limited to simple ratios and normalized difference band ratios (Jackson and Huete, 1991) which we selected to highlight seasonal aspects of the green and dry mix of the tropical pastures (Table 1).

The sensors provided a calibrated numeric output for each spectral band every minute and data volumes were small enough to be transmitted in near real-time via the WSN. After calibrating raw sensor data using individual Skye sensor calibration coefficients, vegetation indices were calculated. It is not possible to calculate reflectance directly from the Skye SKR-1850 sensor. However, Skye provides formulae which use the measured sensitivities of the individual sensors to calculate ratio-style indices such as NDVI (Skye-Instruments, 2012b). These indices are mathematically equivalent to

BGD
12, 18007–18051, 2015

those calculated from reflectance. Using the NDVI example from Skye, we developed formulae for the vegetation indices shown in Table 1.

2.7 Quality control of the sensor data

The types of processing required for high-frequency multispectral time-series are illustrated with an example of a typical diurnal time-series of multispectral data with a reading every minute (Fig. 2). Both raw sensor current and the calculated NDVI values are typically low during the night-time hours. The period of rapidly increasing sensor values at dawn is extremely noisy due to variable early-morning illumination and the scattering of sunlight through a thicker atmosphere at low elevations. At dusk a mirrored pattern of decrease (data not shown), also seen in Weber et al. (2008: Fig. 3a). Apart from the spike in high NDVI values when a green leaf was held in front of the sensor (approximately 13:00), the middle part of the day is the period of relatively stable values of NDVI with random variation compared to the noise in the raw current resulting from variable solar illumination or clouds. To calculate a single daily value from the diurnal cycle of the daily time-series, multi-spectral sensor data, vegetation index values from the middle part of the day (10:00 to 14:00) were selected and the median value calculated to reduce noise due to small fluctuations in illumination.

Data from a particular day were discarded if they met any of the filtering criteria listed in Table 2. Data were not discarded under conditions where changes in the spectral values were considered to be a signal rather than noise. For example, rapid increases over time in values of NDVI corresponded to rapid growth at the start of the wet season. The digital camera images were used as a verification check of the multi-spectral data.

The filtering criteria were developed to screen the daily multi-spectral data series for large fluctuations (Table 2), such as data outliers, spikes, high noise levels, clipping and calibration issues, which can commonly result from anomalies at the sensor or during data transmission (Collins et al., 2006; Ni et al., 2009). For example, the night-time raw current reading should remain relatively constant excluding minor night-time light reflections or electronic noise. Large deviations from night-time baseline current

BGD
12, 18007–18051, 2015

values indicated a technical issue (Table 2, category (a)). The baseline current could also change suddenly if the sensor was swapped for new equipment, or for logistical reasons such as if there was a maintenance ladder underneath the sensor (see Table 2, category (b)). We also developed filtering rules based on the expected spectral response of tropical pastures (see Table 2, category (c)). For example, NDVI for vegetation should not be less than zero (Holben, 1986; Jackson and Huete, 1991). In developing these filtering rules, the vegetation indices stood as proxy for their individual constituent bands as it was not possible to use spectral reflectance from the Skye SKR-1850 sensors directly. Some of the filtering rules excluded valid spectral signals that were not errors, but which were not applicable to our goal of monitoring pastures (Table 2, category (d)). For example, surface water under the vegetation due to heavy rainfall was identified by visual inspection of the camera images combined with the soil moisture data, and filtered because it was not a valid measurement of the pasture status even though it was a valid sensor signal.

2.8 Field measurements of vegetation made under the sensor nodes

Visual observations of pasture biomass (weight of above ground vegetation dry matter (DM) per unit of area) for the sensors FOV were recorded by trained field staff at 2–3 week intervals during the study period. Destructive sampling of the area under the sensors was not desirable as this would have restricted the range of pasture biomass measurements to only low values, and the pastures would not re-grow rapidly enough for accurate visual assessment of biomass if they were cut to ground level. Above-ground standing biomass (kg DM ha^{-1}) (called TotalBiomass henceforth) was therefore assessed by comparing the sensor FOV area with pasture standard photographs. TotalBiomass was not divided into green and dry components as this is difficult to do in this environment, although the green proportion was estimated using the method that follows.

The fraction of bare ground and the fractional coverage by PV (i.e. green) and of NPV (i.e. % dead/dry), are widely used for assessing landscape degradation (Richard-

BGD
12, 18007–18051, 2015

son et al., 2007; Myneni and Williams, 1994; Guerschman et al., 2009). However for a non-expert in remote sensing the fractional cover is a less familiar measurement than TotalBiomass to interpret and use. We made visual field assessments of fractional coverage, by PV (i.e. green) and of NPV (i.e. % dead/dry, as seen in two dimensions from above, across a 1 m by 1 m area under the sensors as follows:

$$\%\,\text{TotalVegetation2D} + \%\,\text{BareGround} + \%\,\text{Litter2D} = 100\,\% \quad (2)$$

where % BareGround is the percentage bare-ground as seen in 2D, % Litter2D is the percentage of litter which is not attached to any plant, and % TotalVegetation2D is the percentage of vegetation still attached to the plant, including both green (PV) and dry (NPV) vegetation as both typically remain on the plant as the plant season during the dry season.

We also visually assessed the percentage of just the visible green proportion of the vegetation, as seen in both two dimensions, looking down at the plot (% Green2D), and three dimensions, looking at the whole plants within the plot (% Green3D). While not as useful as actual measurements of green biomass, these 2-D and 3-D visual assessments give the nearest approximation of green vegetation without destructive samplings and separating green and dry material.

Finally, the area was divided into four quadrants and vegetation height (VegetationHeight, cm) was measured for each of the four quadrants as well as for the total area the height at which 95 % of the vegetation was below, and all five measurements were averaged.

2.9 Model development

To use an indirect sensor measure (e.g. NDVI) to predict biophysical variables (e.g. biomass), it is necessary to model the relationship between the two measurements. Based on the previous work of Handcock et al. (2008) where climate variables were used to improve the performance of the model developed from multi-spectral satellite images and biomass measured by cuts of the temperate dairy pastures, we included

BGD
12, 18007–18051, 2015

a number of climatic variables in our model development: daily minimum and maximum temperature (i.e. T_{Min} and T_{Max}˚C), daily total rainfall (Rain, mm), the accumulated rainfall since the 1 September (i.e. RainAcc-1Sept, mm), soil volumetric water content (i.e. SoilMoisture, %), and the number of days since the 1 January (YearDay).

Model development was restricted to data gathered during the period that is of most interest to cattle producers – from January to April (days 1 to 130 of the year). This period covers the majority of the wet season period of green pasture growth and the critical period at the end of the wet season. These results were also compared to models developed for the dry season (May through December) and to results from across the entire year.

Although previous work in temperate dairy pastures showed saturation of the vegetation indices for high biomass values (Handcock et al., 2008), and this saturation is well supported in the literature (e.g. Sellers, 1985), we did not use non-linear models in the present analysis. This was because visual inspection of the data showed that the relationships between the combinations of dependent and independent variables were linear, making a non-linear model inappropriate. Additionally, the small number of matching time points between the field data and sensor data during the wet season was considered to be too small for developing non-linear relationships.

The least squares linear regression models were developed using the R statistical package (R-Core-Team, 2013) to test how well each biophysical measurement could be predicted from either a single independent sensor variable, or two independent variables where one was sensor derived and one was climate or time related. Indices derived from two sensors, or two multispectral indices, were not combined in the model due to potential correlation between measurements. The independent variables included: vegetation indices derived from the filtered daily dataset from the multi-spectral sensors (i.e. NDVI, gNDVI, NVI-GR, NVI-SR, and RatioNS34) and the digital cameras (i.e. GLA), as well as the daily weather variables (i.e. T_{Min}, T_{Max}, Rain, RainAcc-1Sept, SoilMoisture, YearDay). The dependent variables were; the vi-

BGD
12, 18007–18051, 2015

sual biophysical measurements made at the field sites (TotalBiomass, % BareGround, % Litter2D, % TotalVegetation2D, % Green2D, % Green3D, and VegetationHeight).

After the sensor and field data were filtered to ensure corresponding daily data were available for both the dependent and independent variables, there was not sufficient matching field and multi-spectral data to split the dataset into calibration and validation subsets. We do, however, compare relationships with biophysical values developed for the multi-spectral sensors and the digital cameras, as each provided an independent measurement of the pasture. While this is not ideal, it was a restriction due to the pilot nature of the project and the large amount of data filtering required.

3 Results

3.1 Multi-spectral sensor data

As a result of the rigorous data cleaning using the criteria in Table 2, for the 545 days of data collected at each node, 48 % of days of data from the unfenced node were discarded, and 63 % of days of data from the fenced node were discarded. This large number of filtered days of data reflects the experimental nature of the pilot deployment of the sensors, which resulted in technical and environmental issues with the sensor deployment. However, the rigorous data cleaning we applied was necessary to provide quality data for the model development.

Figure 3 illustrates this data cleaning by showing the time-series of NDVI values from the unfenced node, before (raw) and after filtering. In comparison to the digital cameras, the design of the housing for the Skye SKR-1850 sensors led to significant problems with insects such as mud-wasps nesting in the sensor tubes (Fig. 4 a and b), spiders building webs across the sensor openings, and water ingress below the cosine correction filters which were fitted to the upward pointing sensors.

BGD
12, 18007–18051, 2015

3.2 Field measurements

The field measurements made at each of the two nodes (Fig. 5) illustrate the rapid vegetation growth at the start of the wet season followed by senescence during the dry season. Despite the two nodes being located only 200 m apart, the measurements of TotalBiomass (Fig. 5a) exhibit differences of almost 2000 kg DM ha^{-1} between nodes for the period following the end of the 2011–12 wet-season. The time series of VegetationHeight (Fig. 5b) is less distinctly different between the nodes compared to TotalBiomass, and slowly decreases through the dry-season. In contrast, the observations of % Green2D, and % Green3D (Fig. 5c–d) are comparatively similar between the two nodes.

3.3 Time series of digital camera images and GLA

Over the 545 day study period, the digital cameras captured 22 642 images from the camera mounted at the unfenced node and 23 210 from the fenced node. Data capture from the cameras was more reliable than for the multi-spectral sensors with the loss of only 13 days of data from the unfenced node, and 10 days of data from the fenced node, both due to data card failure.

Figure 6 shows a time series of images from the digital camera at the fenced node, with each 6 week period represented by one image taken at approximately 12:00. The seasonal progression of vegetation is clearly illustrated by these images, from the new green growth of the vegetation at the start of the wet season, followed by senescence during the move into the dry season and the sudden removal of all vegetation following the 2011 controlled-burn. The camera images again illustrate how, as the wet season progresses, the tall grasses dominate the canopy followed by the gradual drying of the canopy in the transition into the dry season.

Figure 7 shows the daily time series of GLA calculated from digital camera images at each node. These results show that the digital cameras and GLA can successfully

BGD
12, 18007–18051, 2015

capture the seasonal changes in green vegetation, corresponding with the rapid growth of green vegetation at the start of the wet season followed by a decrease to zero during the dry season.

3.4 The relationship between sensor data and field estimates

Table 3 shows the regression relationships between field measurements of TotalBiomass and %Green2D (dependent variables) and the sensor-derived GLA, NDVI, and RatioNS34 (independent variables) for data across the whole year, the wet season, and the dry season. Models developed using data from the whole year or for data from outside the wet season performed poorly. For example, with data from the entire year the NDVI explained only 3 % of the variation in TotalBiomass, with a residual standard error (RSE) of 1523 kg DM ha^{-1} (p = 0.308), and the relationship with %Green2D is equally poor (RSE = 2 %, p = 0.368). These results for the dry season are not unexpected given that at that time the pastures contain mainly senesced vegetation, but the spectral bands of the sensors are sensitive to green vegetation. For the relationships with data from across the year this dry-season response is confounded with the discretely different wet season green vegetation growth, as we would expect in a tropical pasture system. Similar outcomes for models developed using data from the whole year or the dry season were found for all combinations of variables (Table 3 shows only selections of these results but all combinations were tested).

In contrast, during the wet season RatioNS34 alone explained 59 % of the variation in TotalBiomass, with an RSE of 1208 kg DM ha^{-1} ($p < 0.01$), and the relationship with %Green2D is equally good (96 % of variation explained, RSE = 5.7 %, $p < 0.01$). Similar outcomes for models developed using data from the wet season were found for all combinations of variables (Table 3 shows only a selection of these results but again all combinations were tested). Based on these results we focus on developing relationships for the wet season.

Table 4 shows the regression relationships for the three top models of wet-season data for each biophysical variable (dependent variable), and models with either a spec-

BGD
12, 18007–18051, 2015

tral index, or a spectral index and climate variable (independent variables). For models with only a single spectral index as the independent variable, both VegetationHeight (independent variable = RatioNS34) and % Green2D (independent variable = RatioNS34) had the strongest relationships, explaining 81 % and 96 % of the variation in the biophysical variables, respectively.

For all other biophysical variables, the 2-variable models with multi-spectral data and the addition of climate data outperformed the 1-variable models explaining greater than 86 % of the variance. The climate variables in these top models were from both weather station data (e.g. RainAcc-1Sept) and from separate sensors on the node (e.g. SoilMoisture). For example, RatioNS34 and RainAcc-1Sept explained 91 % of the variation in TotalBiomass, and RatioNS34 and Rain explained 95 % of the variation in % Green2D. RatioNS34 was the best performing multi-spectral sensor index, being the multi-spectral index included in all of the top ranked 1-variable models and the majority of the top ranked 2-variable models.

Table 5 shows regression relationships for the three top ranked models of wet-season data for each biophysical variable (dependent variable), and models with either only GLA, or GLA and climate variables (independent variables). For models with only GLA as the independent variable, both % Green3D and % Green2D had strong relationships, explaining 83 % and 87 % of the variation in the biophysical variables, respectively. This is expected as GLA is designed to capture the green component of vegetation which is similar to what is captured by assessments of % Green2D and % Green3D.

For all other biophysical variables the top ranked 2-variable models with GLA and the addition of climate data outperformed the 1-variable models, explaining between 50 % and 91 % of the variance, respectively. For example, GLA and SoilMoisture explained 90 % of the variation in % Green3D (RSE = 7 %, $p < 0.01$, df = 16), while GLA and RainAcc-1Sept explained 91 % of the variation in % Green2D (RSE = 9 %, $p < 0.01$, df = 20). Unsurprisingly, the biophysical variable most poorly predicted from GLA was % BareGround, with the top ranked model with YearDay explaining only 50 % of the

BGD
12, 18007–18051, 2015

variation in %BareGround (RSE = 15 %, $p < 0.01$, df = 20). TotalBiomass had weaker relationships with GLA than was found with the multi-spectral indices with the best model with GLA and YearDay explaining only 67 % of the variation in TotalBiomass (RSE = 957 kg DM ha^{-1}, $p < 0.01$, df = 20).

4 Discussion

The tropical pasture conditions in the present study presented unique technical issues that had to be overcome as part of the deployment of proximal sensors, including marked wet and dry seasons, high humidity, rapidly growing vegetation, fire and insects.

4.1 Assessing pasture status

In this study, the time-series of images from the digital cameras and multi-spectral sensors at each node clearly captured the changes in the tropical pastures; from the period of green-up at the start of the wet season, the period of green vegetation growth during the wet season and the gradual senescence and drying-off of the vegetation. Poor relationships between the sensor and field measurements outside of the wet season period are not surprising since NPV is difficult to discern in the NIR spectral region. The lower SWIR band of our multi-spectral sensors was also in the lower part of the SWIR range, which is not as responsive to dry vegetation as the longer SWIR bands.

When combined with climate data, the multi-spectral indices were a better predictor of TotalBiomass than GLA, with the model with RatioNS34 and RainAcc-1Sept explaining 91 % of the variation in TotalBiomass and an RSE of 593 kg DM ha^{-1}. While this RSE is greater than the industry standard in field measurements of a dairy pasture system of approximately 400 kg DM ha^{-1}, although in a temperature pasture (L'Huillier and Thomson, 1988), this result is encouraging for a pilot study.

BGD
12, 18007–18051, 2015

Fractional cover was successfully predicted, with indices calculated from either the multi-spectral sensors or the digital camera data, combined with climate data, explaining high proportions of the variation in %Green2D (95 and 91 % respectively, RSEs of 6 and 9 %, respectively). These strong relationships between the two dimensional variables and field measurements are not unexpected as they both are observed by looking down on the canopy, as different from biomass or %Green3D which are measured in three dimensions.

The multi-spectral sensors were a better predictor of %BareGround than the digital cameras, explaining 90 and 50 % of the variation, respectively (RSEs of 5 and 15 % respectively). These results indicate that while both sensor types are suitable for monitoring aspects of fractional cover in this tropical pasture system, alternative indices extracted from the digital cameras would need to be explored to improve how well %BareGround can be monitored. These results are again not unexpected, as while both sensors view the canopy in two dimensions, the GLA is focussed on the green proportion of the canopy while the band-choice for multi-spectral indices can be made to capture both green and dead aspects of the vegetation.

Fractional cover has the potential to be a valuable part of a multiple data-source approach to providing on-farm data to farmers for sustainable pasture management. Although fractional cover is widely used in landscape degradation studies, particularly in regional monitoring (Richardson et al., 2007; Myneni and Williams, 1994; Guerschman et al., 2009), it is a more recent measurement compared to pasture biomass which has long been used in livestock production systems. Fractional cover is therefore a less familiar measurement than biomass to interpret and use. However, as fractional cover measurements become more widely available (e.g. Guerschman et al., 2009) and examples of its use in operational farm management become available, it is likely that this will change, as occurred when NDVI started to become available for use in agriculture. Sensor nodes could be strategically placed in sensitive areas to monitor areas that are becoming over-grazed, for example to signal an alert to move stock.

BGD
12, 18007–18051, 2015

Due to our stringent data cleaning protocols, which excluded a large amount of data from the multispectral sensors, the models we developed had low degrees of freedom. Future automatic data filtering could also be implemented, for example using spectral data to filter surface water, rather than the manual method we used where we identified surface water using the digital camera images. Our field measurements were made throughout the year, whereas the best models results (Tables 4 and 5) were only for the wet season, when the green vegetation that the spectral bands of the sensors are sensitive to is present. This is compared to the long period of senesced pastures during the dry season which the chosen spectral bands have only limited sensitivity to. Future studies should focus field data collection on the wet season to improve the available data for modelling. This study was run for less than two years, which covers a limited range of pasture conditions as a result of inter-annual variability in climate and differing grazing and pasture management. Further research can be focussed on validating the models. If further studies do not show consistent relationships between sites and years, one option for calibration would be to have the farmer performing a controlled set of calibration measurements once or twice during the growing season to calibrate a particular sensor deployment.

4.2 Comparing camera and multi-spectral sensors

In the extensive database cleaning illustrated in Fig. 3 and Table 2 we focused on post-collection filtering methods, as the experimental nature of our deployment meant that data could not be screened in real time. In an operational system additional rules could be implemented as there are approaches to sensor data cleaning and outlier detection (e.g. Basu and Meckesheimer, 2007; Huemmrich et al., 1999; Liu et al., 2004) including implementing data quality control algorithms within the WSN (e.g. Collins et al., 2006; Jeffery et al., 2006; Zhang et al., 2010). In addition to the data cleaning rules we developed, and as the field deployment progressed, we modified the sensor maintenance protocols and infrastructure. This knowledge can also be used in future deployments.

BGD
12, 18007–18051, 2015

We found the digital cameras to be more robust than the multi-spectral sensors in terms of data flow, with up to 63 % of days of data from our Skye sensors being discarded during data quality control. While the stringent filter criteria (Table 2) may have resulted in some "clean" data being excluded, this was weighed up against the greater impact of having un-trustworthy data for modelling. The long periods of erroneous multi-spectral data made this model of sensor unreliable in this environment. In comparison to the digital camera, the design of the Skye SKR-1850 sensors led to significant problems, including insect infestations in the sensor tubes, and water ingress below the cosine correction filters which were fitted to the upward pointing sensors. While we were able to mitigate the effects of these issues by regular maintenance of the sensors and post-acquisition data cleaning, we found that the Skye SKR-1850 was not stable enough in our tropical environment for an operational deployment on a farm. For example, we had the complete failure of one sensor which then had to be replaced by new equipment. Improved designs for the Skye sensor housing are likely to address many of these issues by having a covered sensor face and also being able to calculate reflectance directly (e.g. the SKR 1860D 4 channel sensor design Skye-Instruments 2013). Repeating this study with the newer sensor design is expected to address many of the issues that we had with the multispectral sensors, so that the focus of future studies will be on gathering multispectral measurements, not on data filtering. In situations where only the earlier model Skye sensors are available, it may be possible to use a method employed by Harris et al. (2014) who were able to overcome similar limitations of earlier models of a SKR-1800 sensor by using a cross-calibration method between the upward- and downward-pointing sensors to retrieve reflectance. While not recommended by the manufacturer, such a method would be useful for deployments where the calibration certificates had expired, or where reflectance was a requirement.

Cross calibration of sensors could also be useful in situations where there is a mix of sensor types deployed to capture spatial variability in the landscape. The growing availability of lower cost sensors provides an alternative to expensive but highly calibrated sensors such as the Skye SKR-1850, with arrays of lower cost sensors relying on mul-

BGD
12, 18007–18051, 2015

tiple sensor redundancy rather than absolute sensor accuracy. Multi-spectral sensors have the potential to be deployed relatively inexpensively if these technical issues can be resolved. In our pilot study the digital camera images were downloaded manually, but as described by Gobbett et al. (2013) in an operational system the cameras could be solar powered and deliver data across a network that had sufficient bandwidth, particularly if daily image capture rather than every 30 min was found to be adequate.

There were benefits to having both multi-spectral sensors and digital cameras as they complement each other in data interpretation. In an operational setting with cost constraints, a single digital camera could be used to give visual feedback on pasture status to the producer, while using a wide deployment of spectral sensors as the main data source. In our study, the climate variables in the top ranked models were from either weather station data or from separate sensors (soil moisture) on the node. A remote sensor node may be enhanced by the addition of a low cost rainfall sensor. However, if sensor setup does not allow for an extra sensor to measure soil moisture or rainfall, these results are encouraging as they indicate that a nearby meteorological station could be used instead.

4.3 Overcoming the limitations of proximal sensors in heterogeneous pastures

An important question about the use of proximal sensors mounted on static nodes is whether the spatial heterogeneity of pastures is adequately captured by the small area on the ground that the sensors observe, assuming an appropriate number of sensors are deployed. The small FOV of an individual sensor is in contrast to the spatially-extensive data obtained from satellite and airborne sensing platforms, and more recently from mobile platforms such as ground vehicles (e.g. King et al., 2010) helicopters, un-manned aerial vehicles (UAV) (e.g. Von Bueren et al., 2015), and robotic setups to move sensors (Hamilton et al., 2007). However, in an operational setting it may not be necessary to spatially sample the landscape exhaustively, as occurs from an imaging platform such as a satellite; the landscape only needs to be sampled suf-

BGD
12, 18007–18051, 2015

ficiently so that the expected spatial variability in the paddock is covered to enable a farm-management decision to be made at critical points in the season.

Options for addressing these spatial sampling concerns of point-based proximal sensors in an operational system include placing multiple sensors strategically in key paddock zones such that the sensors capture the range of paddock variability. Remote sensing images, even if captured only once or twice per year, could be used to aid in the delineation of suitable zones in conjunction with local farmer knowledge. Data from this setup could then be aggregated up to the scale of a farm management unit to create a robust time-series of observations. Alternatively, the sensors could be mounted on a mobile platform that monitors the pastures along a series of waypoints at set times in the day. Unlike the set revisit times of satellite-based remotely sensed images, helicopters and UAVs have the potential for more flexible data capture under cloudy conditions. However, data from these platforms have more complex capture and processing requirements due to the stability of the imaging platform and the capture of strips of image data in separate flight lines. Increasingly, these processing limitations of mobile platforms are being mitigated by advances in automating image processing (Colomina and Molina, 2014), but they still have the limitation of providing intermittent rather than continuous monitoring. More importantly, while capturing raw image data from these systems is relatively easy, creating an operational system to convert the data to something the producer can use for decisions making is more complex.

While there are limitations of using point-based sensors for monitoring heterogeneous tropical pastures, this is balanced by the benefits of having a near real-time continuous data stream for monitoring. For example, an ideal pasture monitoring system would combine data from multiple sources; proximal sensing data for repeated and continuous monitoring of the pastures, and remote sensing images collected at a limited number of times when a spatial assessment of pasture status is required. An automatic sensor system could also be set up to trigger a notification to a smart phone or tablet, when a critical threshold in feed availability or bare-ground has been reached. These data sources could also be combined with other precision farm management

BGD
12, 18007–18051, 2015

technologies, such as walk over weighing (González et al., 2014), and emerging low power sensor network systems (e.g. http://www.taggle.com.au). For these combined sensor technologies to be used on-farm outside of the current research pilot deployment would require future technical development to streamline their installation and operational use.

5 Conclusions

This project successfully gathered proximal sensor data of tropical pastures over 18 months. As this was a pilot deployment of the multiple sensors in this environment we had a number of technical issues that limited the amount of sensor data that was available for comparing to the field measurements. Issues such as insects and dust are common to sensor deployments in all environments, and while mitigated by sensor maintenance, are an issue that would need to be addressed in an automated fashion if multiple autonomous sensors are to be deployed over long time periods. Other issues, such as the gross failure of our multispectral sensor model due to moisture entry were exacerbated by the tropical conditions, but these issues are likely to be greatly reduced in the newer model sensors that have been developed, particularly when choosing low-cost sensor models. Using multispectral sensors with an improved design should provide more robust data collection and require less stringent data filtering. Data processing steps such as noise filtering and the necessity of calibration are common to all spectral sensor deployments, and should be considered part of the operational deployment methodology. Regular maintenance, whether manual or automated, should include re-calibration of sensors due to degradation over time, and the cross-calibration needs of deployments of multiple sensors. Focussing data extraction on the middle part of the day is also common to all sensor deployments, and in an operation setting can be used to limit data acquisition and resource when combined with limiting data acquisition to the critical wet season period of vegetation growth. While we found the digital

BGD
12, 18007–18051, 2015

cameras to be more robust than the multi-spectral sensors in terms of data acquisition, we recommend having a system with both sensor types to aid in data interpretation.

Overall, we found that the limitations of proximal sensors mounted on static nodes are balanced by their ability to monitor continually and deliver near real-time data without being affected by clouds, and their potentially for being deployed autonomously in remote locations in extensive farming systems. Although our pilot deployment of multiple sensors in the tropical environment only had two nodes, during the wet season (January to April) period of maximum pasture growth we found strong relationships between sensor and field measurements. These results show that proximal sensors, particularly when multiple sensors are combined in the same deployment, have the ability to provide a valuable alternative to physical assessments of pasture, particularly as continuous monitoring permits the rapid identification of changing conditions and informed and timely management decision-making on-farm.

Author contribution

The field experiments were designed by RNH (25 %), DLG (25 %), LAG (25 %), and GBH (25 %).

The field work was done by SLM (50 %), LAG (20 %), GBH (20 %), RNH (5 %), and DLG (5 %).

The data cleaning and synthesis was done by RNH (40 %), DLG (35 %), and SLM (25 %).

The design and implementation of the data analysis was done by RNH (50 %) and DLG (50 %).

The manuscript and figures were prepared by RNH (70 %) and DLG (15 %), with contributions from all co-authors, LAG (5 %), GBH (5 %), and SLM (5 %).

Acknowledgements. We gratefully acknowledge the CSIRO Sustainable Agricultural Flagship who funded this research, and Noboru Ota, Chris Crossman, and Philip Valencia for technical support, as well as two anonymous reviewers for their helpful suggestions.

BGD
12, 18007–18051, 2015

References

Allen, M. F., Vargas, R., Graham, E. A., Swenson, W., Hamilton, M., Taggart, M., Harmon, T. C., Rat'Ko, A., Rundel, P., Fulkerson, B., and Estrin, D.: Soil Sensor Technology: Life within a Pixel, Bioscience, 57, 859–867, doi:10.1641/B571008, 2007.

Asner, G. P.: Biophysical and biochemical sources of variability in canopy reflectance, Remote Sens. Environ., 64, 134–153, 1998.

Balzarolo, M., Anderson, K., Nichol, C., Rossini, M., Vescovo, L., Arriga, N., Wohlfahrt, G., Calvet, J.-C., Carrara, A., Cerasoli, S., Cogliati, S., Daumard, F., Eklundh, L., Elbers, J. A., Evrendilek, F., Handcock, R. N., Kaduk, J., Klumpp, K., Longdoz, B., Matteucci, G., Meroni, M., Montagnani, L., Ourcival, J.-M., Sánchez-Cañete, E. P., Pontailler, J.-Y., Juszczak, R., Scholes, B., and Martín, M. P.: Ground-based optical measurements at European flux sites: A review of methods, instruments and current controversies, Sensors, 11, 7954–7981, 2011.

Basu, S. and Meckesheimer, M.: Automatic outlier detection for time series: An application to sensor data, Knowl. Inf. Syst., 11, 137–154, 2007.

Bennett, L. T., Judd, T. S., and Adams, M. A.: Close-range vertical photography for measuring cover changes in perennial grasslands, J. Range Manage., 53, 634–641, doi:10.2307/4003159, 2000.

Booth, D. T., Cox, S. E., Fifield, C., Phillips, M., and Willlamson, N.: Image analysis compared with other methods for measuring ground cover, Arid Land Res. Manag., 19, 91–100, 2005.

Collins, S. L., Bettencourt, L. M. A., Hagberg, A., Brown, R. F., Moore, D. I., Bonito, G., Delin, K. A., Jackson, S. P., Johnson, D. W., Burleigh, S. C., Woodrow, R. R., and McAuley, J. M.: New opportunities in ecological sensing using wireless sensor networks, Front. Ecol. Environ., 4, 402–407, 2006.

Colomina, I. and Molina, P.: Unmanned aerial systems for photogrammetry and remote sensing: A review, ISPRS J. Photogramm., 92, 79–97, doi:10.1016/j.isprsjprs.2014.02.013, 2014.

Eklundh, L., Jin, H., Schubert, P., Guzinski, R., and Heliasz, M.: An optical sensor network for vegetation phenology monitoring and satellite data calibration, Sensors, 11, 7678–7709, doi:10.3390/s110807678, 2011.

Ewing, R. P. and Horton, R.: Quantitative color image analysis of agronomic images, Agron. J., 91, 148–153, 1999.

BGD
12, 18007–18051, 2015

Gamon, J. A.: Reviews and Syntheses: optical sampling of the flux tower footprint, Biogeosciences, 12, 4509–4523, doi:10.5194/bg-12-4509-2015, 2015.
Gitelson, A. A., Kaufman, Y. J., and Merzlyak, M. N.: Use of a green channel in remote sensing of global vegetation from EOS–MODIS, Remote Sens. Environ., 58, 289–298, 1996.
Gobbett, D., Handcock, R. N., Zerger, A., Crossman, C., Valencia, P., Wark, T., and Davies, M.: Prototyping an Operational System with Multiple Sensors for Pasture Monitoring, J ournal of Sensor and Actuator Networks, 2, 388–408, 2013.
González, L. A., Bishop-Hurley, G., Henry, D., and Charmley, E.: Wireless sensor networks to study, monitor and manage cattle in grazing systems, Anim. Prod. Sci., 54, 1687–1693, doi:10.1071/AN14368, 2014.
Guerschman, J. P., Hill, M. J., Renzullo, L. J., Barrett, D. J., Marks, A. S., and Botha, E. J.: Estimating fractional cover of photosynthetic vegetation, non-photosynthetic vegetation and bare soil in the Australian tropical savanna region upscaling the EO-1 Hyperion and MODIS sensors, Remote Sens. Environ., 113, 928–945, doi:10.1016/j.rse.2009.01.006, 2009.
Hamilton, M. P., Graham, E. A., Rundel, P. W., Allen, M. F., Kaiser, W., Hansen, M. H., and Estrin, D. L.: New Approaches in Embedded Networked Sensing for Terrestrial Ecological Observatories, Environmental Engineering Science, 24, 192–204, doi:10.1089/ees.2006.0045, 2007.
Handcock, R. N., Mata, G., and Gherardi, S. G.: Combining spectral information aggregated to the paddock scale with knowledge of on-farm practices will enhance remote sensing methods for intensively managed dairy pastures, 14th Australian Remote Sensing and Photogrammetry Conference, Darwin, Australia, 29 September–3 October 2008, 2008.
Harris, A., Gamon, J. A., Pastorello, G. Z., and Wong, C. Y. S.: Retrieval of the photochemical reflectance index for assessing xanthophyll cycle activity: a comparison of near-surface optical sensors, Biogeosciences, 11, 6277–6292, doi:10.5194/bg-11-6277-2014, 2014.
Holben, B. N.: Characteristics of maximum-value composite images from temporal AVHRR data, Int. J. Remote Sens., 7, 1417–1434, doi:10.1080/01431168608948945, 1986.
Huemmrich, K. F., Black, T. A., Jarvis, P. G., McCaughey, J. H., and Hall, F. G.: High temporal resolution NDVI phenology from micrometeorological radiation sensors, J. Geophys. Res., 104, 27935–27944, doi:10.1029/1999JD900164, 1999.
Jackson, R. D. and Huete, A. R.: Interpreting vegetation indices, Prev. Vet. Med., 11, 185–200, doi:10.1016/S0167-5877(05)80004-2, 1991.

BGD
12, 18007–18051, 2015

Jeffery, S. R., Alonso, G., Franklin, M. J., Wei, H., and Widom, J. A.: Pipelined Framework for Online Cleaning of Sensor Data Streams, 22nd International Conference on Data Engineering, ICDE'06, Atlanta, USA, 3–7 April 2006, 2006.

Johnson, D., Vulfson, M., Louhaichi, M., and Harris, N.: Vegmeasure v1.6 user's manual, Department of Rangeland Resources, Oregon State University, Corvallis, Oregon, USA, 2003.

Karcher, D. E. and Richardson, M. D.: Batch analysis of digital images to evaluate turfgrass characteristics, Crop. Sci., 45, 1536–1539, 2005.

King, W., Rennie, G. M., Dalley, D. E., Dynes, R. A., and Upsdell, M. P.: Pasture mass estimation by the C-DAX pasture meter: regional calibrations for New Zealand, in: Proceedings of the Australasian Dairy Science Symposium, Caxton Press, 31 August to 2 September 2010, Lincoln University, New Zealand, 233–238, 2010.

L'Huillier, P. J. and Thomson, N. A.: Estimation of herbage mass in ryegrass/white clover dairy pastures, New Zealand Grassland Association Conference Balclutha, New Zealand, 1988.

Liu, H., Shah, S., and Jiang, W.: On-line outlier detection and data cleaning, Comput. Chem. Eng., 28, 1635–1647, 2004.

Lo, F., Wheeler, M. C., Meinke, H., and Donald, A.: Probabilistic forecasts of the onset of the north Australian wet season, Mon. Weather Rev., 135, 3506–3520, 2007.

Louhaichi, M., Borman, M. M., and Johnson, D. E.: Spatially located platform and aerial photography for documentation of grazing impacts on wheat, Geocarto International, 16, 65–70, 2001.

Lukina, E. V., Stone, M. L., and Raun, W. R.: Estimating vegetation coverage in wheat using digital images, J. Plant. Nutr., 22, 341–350, 1999.

Myneni, R. B. and Williams, D. L.: On the relationship between FAPAR and NDVI, Remote Sens. Environ., 49, 200-211, 1994.

Ni, K., Ramanathan, N., Chehade, M. N. H., Balzano, L., Nair, S., Zahedi, S., Kohler, E., Pottie, G., Hansen, M., and Srivastava, M.: Sensor network data fault types, ACM T. Sensor. Network., 5, 1–29, 2009.

O'Reagain, P., Scanlan, J., Hunt, L., Cowley, R., and Walsh, D.: Sustainable grazing management for temporal and spatial variability in north Australian rangelands - A synthesis of the latest evidence and recommendations, Rangeland J., 36, 223–232, doi:10.1071/RJ13110, 2014.

Pearson, R. L., Tucker, C. J., and Miller, L. D.: Spectral mapping of shortgrass prairie biomass, Photogramm. Eng. Rem. S., 42, 317–323, 1976.

BGD
12, 18007–18051, 2015

Peddle, D. R., Peter White, H., Soffer, R. J., Miller, J. R., and LeDrew, E. F.: Reflectance processing of remote sensing spectroradiometer data, Comput. Geosci., 27, 203–213, doi:10.1016/S0098-3004(00)00096-0, 2001.
Richardson, A. D., Jenkins, J. P., Braswell, B. H., Hollinger, D. Y., Ollinger, S. V., and Smith, M. L.: Use of digital webcam images to track spring green-up in a deciduous broadleaf forest, Oecologia, 152, 323–334, 2007.
Sakowska, K., Vescovo, L., Marcolla, B., Juszczak, R., Olejnik, J., and Gianelle, D.: Monitoring of carbon dioxide fluxes in a subalpine grassland ecosystem of the Italian Alps using a multispectral sensor, Biogeosciences, 11, 4695–4712, doi:10.5194/bg-11-4695-2014, 2014.
Sanderson, M. A., Rotz, C. A., Fultz, S. W., and Rayburn, E. B.: Estimating Forage Mass with a Commercial Capacitance Meter, Rising Plate Meter, and Pasture Ruler, Agron. J., 93, 1281–1286, doi:10.2134/agronj2001.1281, 2001.
Sellers, P. J.: Canopy reflectance, photosynthesis and transpiration, Int. J. Remote Sens., 6, 1335–1372, 1985.
Skye-Instruments: SKR 1850D and 1850ND, SKR 1850D/A and 1850ND/A 4 Channel Sensor, 21, Ddole Enterprise Park, Llandrindod Wells, Powys LD1 6DF, UK, 1, 2012a.
Skye-Instruments: Application Notes Sensors for NDVI Calculations, 21, Ddole Enterprise Park, Llandrindod Wells, Powys LD1 6DF, UK, 1, 2012b.
Skye-Instruments: 4 Channel Sensor SKR 1860D and SKR 1860ND, 21, Ddole Enterprise Park, Llandrindod Wells, Powys LD1 6DF, UK, 1, 2013.
Szewczyk, R., Osterweil, E., Polastre, J., Hamilton, M., Mainwaring, A., and Estrin, D.: Habitat monitoring with sensor networks, Communications of the ACM, 47, 34–40, doi:10.1145/990680.990704, 2004.
Tucker, C. J.: Red and photographic infrared linear combinations for monitoring vegetation, Remote Sens. Environ., 8, 127–150, 1979.
Tucker, C. J.: Remote sensing of leaf water content in the near infrared, Remote Sens. Environ., 10, 23–32, 1980.
Turner, D. P., Cohen, W. B., Kennedy, R. E., Fassnacht, K. S., and Briggs, J. M.: Relationships between leaf area index and Landsat TM spectral vegetation indices across three temperate zone sites, Remote Sens. Environ., 70, 52–68, 1999.
von Bueren, S. K., Burkart, A., Hueni, A., Rascher, U., Tuohy, M. P., and Yule, I. J.: Deploying four optical UAV-based sensors over grassland: challenges and limitations, Biogeosciences, 12, 163–175, doi:10.5194/bg-12-163-2015, 2015.

BGD
12, 18007–18051, 2015

Weber, C., Schinca, D. C., Tocho, J. O., and Videla, F.: Passive field reflectance measurements, J. Opt. A.-Pure. Appl. Op., 10, 104020, 2008.

Zerger, A., Viscarra Rossel, R. A., Swain, D. L., Wark, T., Handcock, R. N., Doerr, V. A. J., Bishop-Hurley, G. J., Doerr, E. D., Gibbons, P. G., and Lobsey, C.: Environmental sensor networks for vegetation, animal and soil science, Int. J. Appl. Earth. Obs., 12, 302–316, doi:10.1016/j.jag.2010.05.001, 2010.

Zerger, A., Gobbett, D., Crossman, C., Valencia, P., Wark, T., Davies, M., Handcock, R. N., and Stol, J.: Temporal monitoring of groundcover change using digital cameras, Int. J. Appl. Earth Obs., 19, 266–275, 2012.

Zhang, Y., Meratnia, N., and Havinga, P. J. M.: Ensuring high sensor data quality through use of online outlier detection techniques, International Journal of Sensor Networks, 7, 141–151, 2010.

BGD
12, 18007–18051, 2015

Table 1. Vegetation indices calculated from the multi-spectral sensor data. ρ = reflectance (0 to 1).

Index Name	Equation	Reference
NDVI	$(\rho_{NIR} - \rho_{red})/(\rho_{NIR} + \rho_{red})$	(Tucker, 1979)
RatioNS34	$\rho_{NIR}/\rho_{lowerSWIR}$	A broadband ratio index (e.g. Handcock et al., 2008)
NVI-GR	$(\rho_{green} - \rho_{red})/(\rho_{green} + \rho_{red})$	A generic broadband normalized ratio index (Jackson and Huete, 1991)
gNDVI	$(\rho_{NIR} - \rho_{green})/(\rho_{NIR} + \rho_{green})$	(Gitelson et al., 1996)
NVI-SR	$(\rho_{lowerSWIR} - \rho_{red})/(\rho_{lowerSWIR} + \rho_{red})$	A generic broadband normalized ratio index (Jackson and Huete, 1991)

BGD
12, 18007–18051, 2015

Table 2. Criteria for filtering multi-spectral data for a day. Daily data were removed if they met any one of the following criteria.

Filtering Category	Data source	Criteria for deleting that day's data.
(a) Spike in readings or readings out of range, such as from a sensor issue	Night-time (00:00 to 01:00) median value of raw current.	One or more of the multi-spectral sensor bands in the paired node has a night-time median value of raw current > 10 000 mV.
		One or more of the multi-spectral sensor bands (raw current) in the paired node is > 3 STD from the band mean value.
	Day-time (12:00 to 13:00) median value of indices.	Data out of range (i.e. NDVI < 0.1) (Holben, 1986; Jackson and Huete, 1991).
(b) Physical/logistical	Project metadata.	Work being done in the area under the node, sensors have been removed for maintenance or because the paddocks are being burned etc.
(c) Tests of spectral indices	Day-time (12:00 to 13:00) median value of indices.	There are no data available during the midday period from one or more of the sensors, which would restrict the calculation of a full suite of indices.
		NDVI < 0 (not likely in tropical pastures).
		RatioNS34 > 2, indicating a technical error as pastures should not have values in this range.
		RatioNS34 drops to zero briefly then returns to previous value, indicating a technical error with the sensor.
		(gNDVI < 0 or NVI-GR > −0.10) and the date and weather data indicates that is in the dry season (i.e. the changing values are unlikely due to surface water.
(d) Masking valid spectral data	Digital camera images, project metadata, and soil moisture data.	Surface water was identified by a combination of data sources and masked as it confounded the pasture signal.

BGD
12, 18007–18051, 2015

Table 3. Linear regression statistics for models with a single independent variable. RSE units are % for % Green2D, and kg DM ha^{-1} for TotalBiomass.

Period	Model	RSE	df	R^2	p value
all year	% Green2D = −10.19 × NDVI + 16.73	13.2	40	0.02	0.368
dry	% Green2D = 158.73 × NDVI − 26.19	22.8	30	0.50	0.000
wet	% Green2D = 129.24 × NDVI − 16.92	11.6	8	0.82	0.000
all year	% Green2D = −25.95 × RatioNS34 + 45.5	30.9	30	0.08	0.122
dry	% Green2D = −25.95 × RatioNS34 + 45.5	30.9	30	0.08	0.122
wet	% Green2D = 279.61 × RatioNS34 − 201.89	5.7	8	0.96	0.000
all year	% Green2D = 192.24 × GLA + 5.626	13.7	37	0.79	0.000
dry	% Green2D = 192.24 × GLA + 5.626	13.7	37	0.79	0.000
wet	% Green2D = 74.344 × GLA + 23.155	10.4	21	0.87	0.000
all year	TotalBiomass = 2016.6 × NDVI + 1751	1523	30	0.03	0.308
dry	TotalBiomass = 2016.6 × NDVI + 1751	1523	30	0.03	0.308
wet	TotalBiomass = 6214 × NDVI − 1459	1469	8	0.40	0.051
all year	TotalBiomass = −134.6 × RatioNS34 + 2501.3	1549	30	0.00	0.870
dry	TotalBiomass = −134.6 × RatioNS34 + 2501.3	1549	30	0.00	0.870
wet	TotalBiomass = 15199 × RatioNS34 − 11977	1208	8	0.59	0.009
all year	TotalBiomass = 3811 × GLA + 2138	1409	37	0.12	0.030
dry	TotalBiomass = 3811 × GLA + 2138	1409	37	0.12	0.030
wet	TotalBiomass = 2441 × GLA + 1040.8	1351	21	0.30	0.007

BGD
12, 18007–18051, 2015

Table 4. Linear regression statistics for the three best models of wet-season data for each biophysical variable (dependent variable) and (a) models with one spectral index, and (b) models with one spectral index and one climate variable. RSE units are kg DM ha^{-1} for TotalBiomass, cm for VegetationHeight, and % for the other dependent variables.

Biophysical	(a) Model (spectral)	RSE	df	R^2	p value
TotalBiomass	15 199 × RatioNS34 – 11977	1208.0	8	0.59	0.009
	6214 × NDVI – 1459	1469.0	8	0.40	0.051
	10 464 × gNDVI – 4049	1487.0	8	0.38	0.057
VegetationHeight	227.71 × RatioNS34 – 170.93	10.6	8	0.81	0.000
	107.46 × NDVI – 21.55	12.7	8	0.72	0.002
	164.745 × NVI-GR + 39.865	13.8	8	0.68	0.004
% Green3D	290.13 × RatioNS34 – 202.47	11.3	8	0.86	0.000
	243.31 × gNDVI – 76.68	12.7	8	0.82	0.000
	139.31 × NDVI – 13.51	13.6	8	0.79	0.001
% Green2D	279.61 × RatioNS34 – 201.89	5.7	8	0.96	0.000
	129.24 × NDVI – 16.92	11.6	8	0.82	0.000
	220.61 × gNDVI – 72.53	11.9	8	0.81	0.000
% TotalVegetation2D	240.3 × RatioNS34 – 154.48	17.1	8	0.64	0.005
	107.836 × NDVI + 6.334	19.9	8	0.52	0.018
	180.35 × gNDVI – 37.88	20.4	8	0.49	0.023
% Litter2D	−108.44 × RatioNS34 + 114.61	11.7	8	0.44	0.036
	−85.696 × NVI-GR + 14.214	11.7	8	0.44	0.037
	−50.92 × NDVI + 43.32	12.2	8	0.39	0.053
% BareGround	−129.2 × RatioNS34 + 137.91	9.9	8	0.61	0.008
	−102.6 × gNDVI + 78.52	10.9	8	0.52	0.018
	−55.94 × NDVI + 50.28	11.7	8	0.46	0.031

BGD
12, 18007–18051, 2015

Table 4. Continued.

Biophysical	(b) Model (spectral + climate)	RSE	df	R^2	p value
TotalBiomass	2834.31 × RatioNS34 + 3.10 × RainAcc-1Sept – 2524.45	593	7	0.91	0.000
	980.24 × NVI-GR + 3.38 × RainAcc-1Sept – 78.78	615	7	0.91	0.000
	337.90 × NDVI + 3.41 × RainAcc-1Sept – 293.67	622	7	0.91	0.000
VegetationHeight	236.72 × RatioNS34 – 1.70 × Rain – 175.55	5.7	7	0.95	0.000
	117.86 × NDVI – 2.06 × Rain – 22.98	7.0	7	0.93	0.000
	205.10 × gNDVI – 2.42 × Rain – 75.18	7.5	7	0.92	0.000
% Green3D	183.75 × NVI-SR – 0.78 × SoilMoisture – 31.55	8.4	4	0.92	0.007
	131.70 × NDVI – 0.38 × SoilMoisture + 0.45	8.4	4	0.92	0.007
	239.96 × gNDVI – 0.51 × SoilMoisture – 65.33	8.0	4	0.92	0.006
% Green2D	236.72 × RatioNS34 – 1.70 × Rain – 175.55	5.7	7	0.95	0.000
	117.86 × NDVI – 2.06 × Rain – 22.98	7.0	7	0.93	0.000
	205.10 × gNDVI – 2.42 × Rain – 75.18	7.5	7	0.92	0.000
% TotalVegetation2D	360.77 × RatioNS34 – 3.496 × SoilMoisture – 222.80	11.2	4	0.90	0.011
	332.866 × NVI-GR – 4.878 × SoilMoisture + 136.58	12.4	4	0.87	0.016
	163.146 × NVI-GR – 6.409 × T_{Min} + 206.36	11.7	7	0.86	0.001
% Litter2D	−61.13 × NDVI + 2.019 × Rain + 44.721	6.3	7	0.86	0.001
	−80.68 × NVI-SR + 2.109 × Rain + 59.137	6.5	7	0.85	0.001
	−118.14 × RatioNS34 + 1.825 × Rain + 119.59	6.8	7	0.83	0.002
% BareGround	−159.02 × RatioNS34 + 1.162 × SoilMoisture + 148.21	5.0	4	0.90	0.010
	−86.55 × NDVI + 1.576 × SoilMoisture + 43.69	5.0	4	0.90	0.010
	−76.95 × RatioNS34 + 3.668 × T_{Max} – 26.474	5.4	7	0.90	0.000

BGD
12, 18007–18051, 2015

Table 5. Linear regression statistics for the three top performing models of wet-season data for each biophysical variable (dependent variable) and (a) models with GLA, and (b) models with GLA and one climate variable. RSE units are kg DM ha^{-1} for TotalBiomass, cm for VegetationHeight, and % for the other dependent variables.

Biophysical variable	(a) Model (GLA)	RSE	df	R^2	p value
TotalBiomass	2441.6 × GLA + 1040.8	1351.0	21	0.30	0.007
VegetationHeight	52.163 × GLA + 18.859	17.2	21	0.55	0.000
% Green3D	61.472 × GLA + 39.181	10.3	21	0.83	0.000
% Green2D	74.344 × GLA + 23.155	10.4	21	0.87	0.000
% TotalVegetation2D	61.457 × GLA + 37.364	17.3	21	0.63	0.000
% Litter2D	−25.245 × GLA + 26.378	10.3	21	0.44	0.001
% BareGround	−36.345 × GLA + 36.725	16.2	21	0.40	0.001

BGD
12, 18007–18051, 2015

Table 5. Continued.

Biophysical variable	(b) Model (GLA + climate)	RSE	df	R^2	p value
TotalBiomass	509.204 × GLA + 35.661 × YearDay + 350.34	956.7	20	0.67	0.000
	907.013 × GLA + 2.316 × RainAcc-1Sept + 473.932	1102.0	20	0.56	0.000
	2667.67 × GLA – 167.88 × Rain + 1310.21	1116.0	20	0.55	0.000
VegetationHeight	54.968 × GLA – 2.084 × Rain + 22.203	14.4	20	0.70	0.000
	41.026 × GLA + 0.206 × YearDay + 14.88	16.7	20	0.60	0.000
	44.396 × GLA + 0.012 × RainAcc-1Sept + 15.99	17.1	20	0.57	0.000
% Green3D	57.917 × GLA – 0.174 × SoilMoisture + 46.62	7.1	16	0.90	0.000
	53.066 × GLA + 0.013 × RainAcc-1Sept + 36.076	9.5	20	0.86	0.000
	53.806 × GLA + 0.141 × YearDay + 36.442	9.8	20	0.85	0.000
% Green2D	63.352 × GLA + 0.017 × RainAcc-1Sept + 19.095	8.8	20	0.91	0.000
	63.189 × GLA + 0.206 × YearDay + 19.169	8.9	20	0.91	0.000
	75.813 × GLA – 1.09 × Rain + 24.905	9.2	20	0.90	0.000
% TotalVegetation2D	38.298 × GLA + 0.427 × YearDay + 29.089	13.0	20	0.80	0.000
	64.565 × GLA – 2.308 × Rain + 41.068	13.7	20	0.78	0.000
	43.318 × GLA + 0.027 × RainAcc-1Sept + 30.664	14.7	20	0.74	0.000
% Litter2D	−27.354 × GLA + 2.456 × T_{min} – 27.108	8.8	20	0.61	0.000
	−15.415 × GLA – 0.015 × RainAcc-1Sept + 30.009	9.1	20	0.59	0.000
	−15.067 × GLA – 0.188 × YearDay + 30.015	9.2	20	0.58	0.000
% BareGround	−23.629 × GLA – 0.235 × YearDay + 41.268	15.2	20	0.50	0.001
	−38.112 × GLA + 1.312 × Rain + 34.619	15.3	20	0.49	0.001
	−28.328 × GLA – 0.012 × RainAcc-1Sept + 39.686	16.0	20	0.44	0.003

BGD
12, 18007–18051, 2015

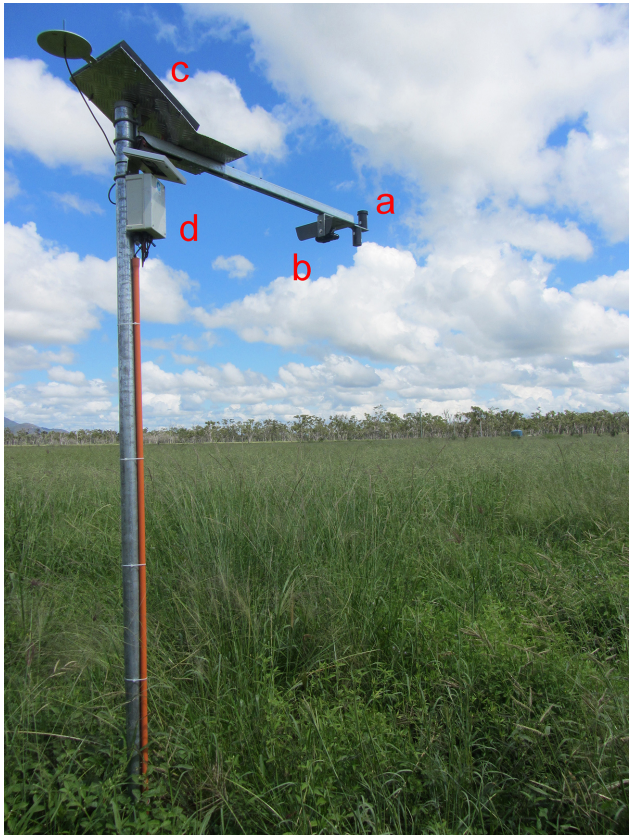

Figure 1. The unfenced node with (a) the paired multi-spectral sensors with the cosine diffusion filter fitted only to the upward-pointing sensor, (b) the digital camera, (c) solar panel power supply, and (d) relay hardware to send data to the WSN.

BGD
12, 18007–18051, 2015

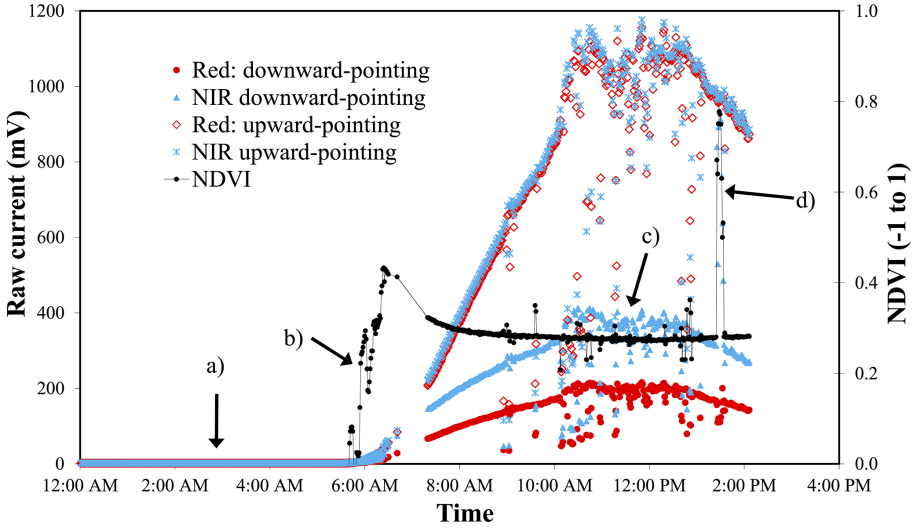

Figure 2. Example of the diurnal cycle of sensor data during the dry season when a large green leaf was held up to the multi-spectral sensors on the fenced node to test its response (4 October 2011). Note: for the NDVI values **(a)** night-time values, **(b)** the ramp-up after dawn (approx. 6:30 a.m.), **(c)** the relatively stable values for the middle part of the day, **(d)** the spike in NDVI when the sensors recorded an elevation of NIR reflectance in response to green vegetation being held up to the sensor.

BGD
12, 18007–18051, 2015

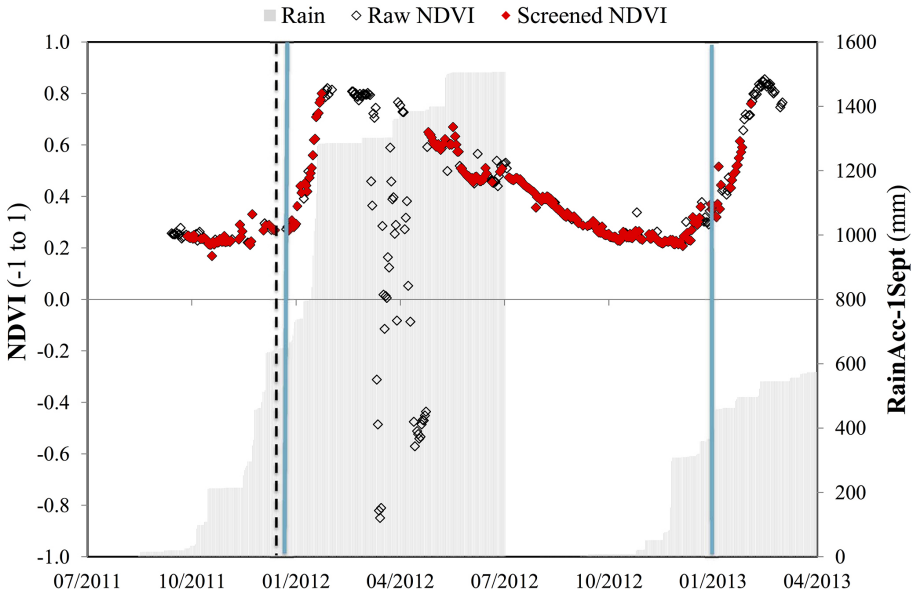

Figure 3. Time-series of NDVI values from the unfenced node showing the raw and screened NDVI and the accumulated precipitation since 1 September (mm) from "Townsville Airport" BoM weather station. The black dashed vertical line indicates the timing of the controlled burn, and the blue lines the start of the wet seasons.

BGD
12, 18007–18051, 2015

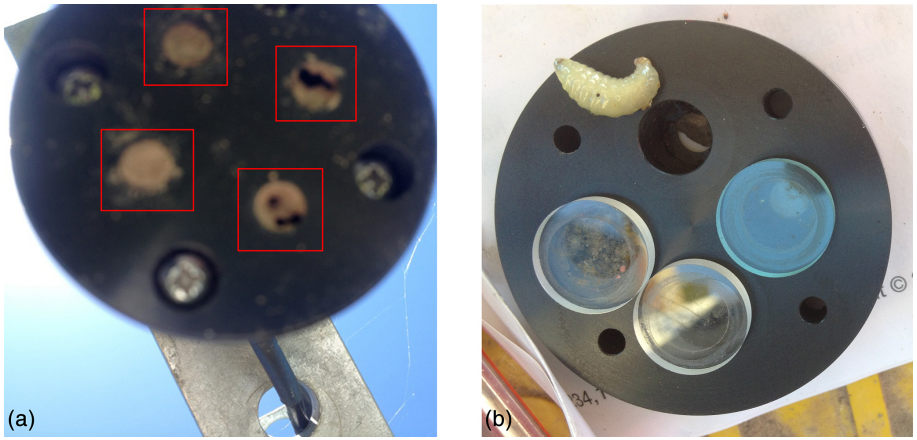

Figure 4. Skye multi-spectral sensors showing **(a)** mud wasps, and **(b)** wasp larvae in sensor tubes.

BGD
12, 18007–18051, 2015

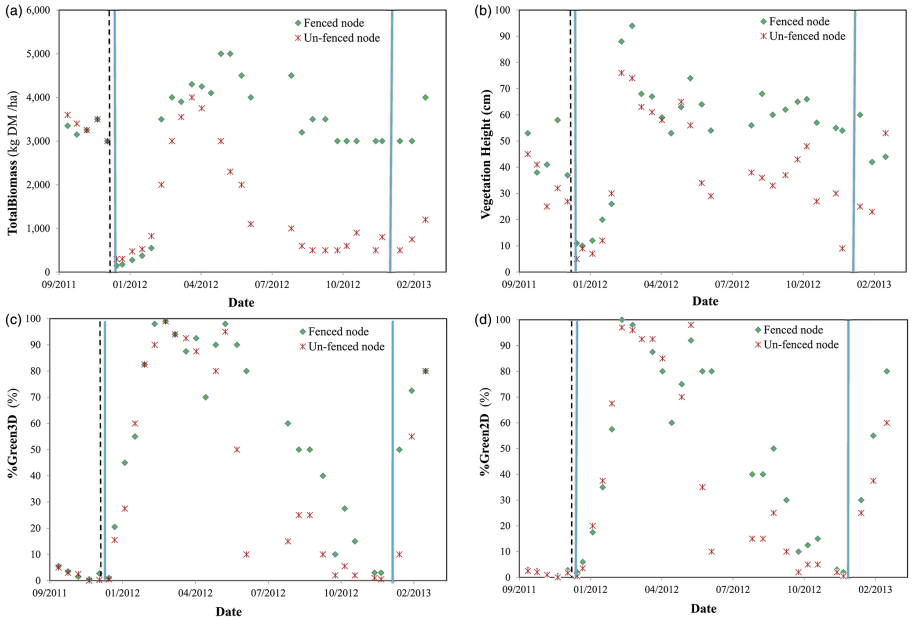

Figure 5. Field observation time series from the two nodes of **(a)** TotalBiomass, **(b)** Vegetation-Height, **(c)** % Green3D, and **(d)** % Green2D. The black dashed line indicates the timing of the controlled burn, and the blue lines the start of the wet seasons.

BGD
12, 18007–18051, 2015

Figure 6. Time series of a year of images from the digital camera at the fenced node, with each 6 week period represented by one image from approximately noon. Dates represent the start of the 6-week period. The red line indicates the controlled burn in December 2011.

BGD
12, 18007–18051, 2015

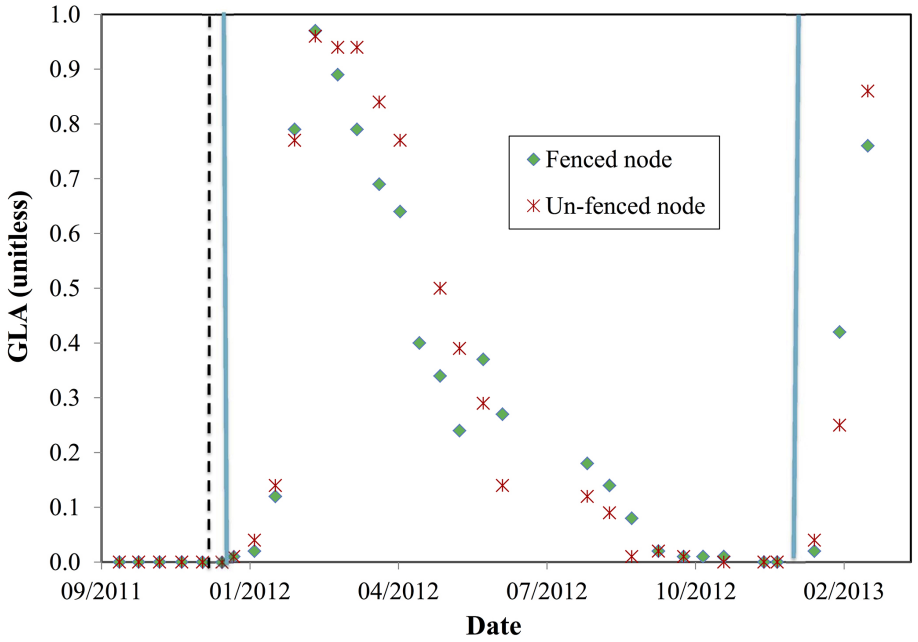

Figure 7. Time series of the Green Leaf Algorithm (GLA) calculated from digital camera images at each node, using a daily image from approximately 12:00. The black dashed vertical line indicates the timing of the controlled burn, and the blue lines the start of the wet seasons.

BGD
12, 18007–18051, 2015